

SYNTHESIS AND PHOTOLUMINESCENCE STUDY OF PVA –CAPPED ZnS:Mn²⁺ NANOPARTICLES

G. MURUGADOSS*, B. RAJAMANNAN, V. RAMASAMY

Department of Physics, Annamalai University, Annamalainagar Tamilnadu, India -608 002

Photoluminescence properties of polyvinyl alcohol (PVA) capped ZnS:Mn²⁺ nanoparticles are reported. The particles were synthesized using chemical precipitation method. The nanoparticles are characterized by X-ray diffraction (XRD), transmission electron microscopy (TEM), ultraviolet-visible (UV/Vis) and photoluminescence (PL). XRD and TEM studies show the formation of cubic PVA-ZnS:Mn²⁺ particles with an average size of ~3 nm. The capped ZnS:Mn²⁺ nanoparticles showed enhanced luminescence property compared with that of the uncapped ZnS:Mn²⁺ particles.

(Received March 15, 2010; accepted April 20, 2010)

Keywords: Semiconductor materials, Chemical synthesis, Photoluminescence, TEM, PVA

1. Introduction

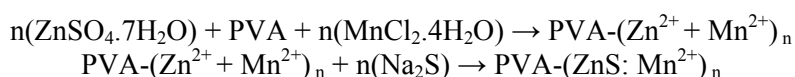
Recently, nanostructured functional materials have attracted much research interest due to their remarkable size, shape and surface dependent physical and chemical properties [1,2]. Zinc sulphide (ZnS), a wide band gap II–VI compound semiconductor is very much promising material for its wide applications in electroluminescence and optoelectronic devices. Various chemical and physical techniques are employed to investigate the optical properties of nanocrystalline ZnS [3–6]. The electronic properties of nanosized ZnS are also strongly influenced by doping of transition and rare earth metals [7, 8]. The emission efficiency and thermal stability increased upon reduction of ZnS particle size [9–11]. The confinement of electrons within nanodimension leads to unusual behavior. The introduction of surface states with miniaturization of sample size also affects the electronic energy states of wide band gap semiconductor. The optical properties of ZnS nanoparticles can be tuned by passivating surfaces with different organic molecules.

The ZnS doped with manganese has been studied intensively as an important electroluminescence material. Because of the high solubility of Mn in zinc sulphide [12], this material can readily be doped, which is one of the reasons for the application of ZnS:Mn²⁺ in electroluminescence thin-film displays [13]. It is supposed that Mn²⁺ ions occupy cation positions in the zinc sulphide lattice [14]. However, the degree of homogeneity of Mn²⁺ ions is essential for achieving luminescence with high efficiency even in the nanocrystallites of ZnS:Mn²⁺ [15]. Bhargava et al. [9] reported for the first time that Mn-doped ZnS nanosized particle which can be prepared by reacting diethylzinc and diethylmanganese with H₂S in toluene. Nien et al. prepared ZnS:Mn²⁺ nanoparticles by a new chemical process applying a mixture of zinc nitrate and manganese nitrate with Na₂S in de-ionized water and sodium hexametaphosphate (SHMP) as a surfactant.

The aim of this work is to study the influence of polyvinyl alcohol (PVA) in ZnS:Mn²⁺ preparation using chemical precipitation method.

2. Experimental

To synthesize ZnS:Mn²⁺ nanoparticles the chemicals used were ZnSO₄·7H₂O, MnCl₂·4H₂O, polyvinyl alcohol (PVA) and Na₂S. In a typical procedure, aqueous stock solutions of (1M) 7.4g of ZnSO₄·7H₂O, and different concentrations (0.5, 1.0, 1.5, 2.0 and 2.5) of surfactants were dissolved in 50 ml doubled distilled water under vigorously stirring, then 0.3g (4%) of 10 ml MnCl₂·4H₂O was added to the above solution. Finally, 2.75g (0.5M) of 50 ml Na₂S solution was introduced into the above solution under continuous stirring. During the whole reaction process, the reactants were vigorously stirred at 80°C for 1h. Then cooled to room temperature, the solution with white flocculent precipitate is appeared. The precipitate was cleaned repeatedly with deionized water and ethanol. Finally, the powder is dried at 60°C under vacuum for two hour. The reactions take place as followed:



XRD patterns of the ZnS:Mn²⁺ samples were recorded using XPERT-PRO diffractometer with a Cu K α radiation ($\lambda=1.54060 \text{ \AA}$) under the same conditions. The crystallite size was estimated using the Scherer equation ($k\lambda$)/ ($\beta \cos\theta$) at the full-width at half-maximum of the major XRD peak. The size and morphology of the particles were determined using TEM (PHILIPS-CM200; 20-200kV). For sample preparation, dilute drops of suspension were allowed to dry slowly on carbon-coated copper grids for TEM. The optical transmission/absorption spectra of the same particles in de-ionized water were recorded using UV-1650PC SHIMADZU spectrometer. Fluorescence measurements were performed on a RF-5301PC spectrophotometer. Emission (350-700 nm) spectra were recorded under 300 nm.

3. Results and discussion

Fig. 1 illustrates the XRD patterns of uncapped and PVA –capped ZnS:Mn²⁺ nanoparticles. It shows three diffraction peaks (2θ) of 29.20, 47.5 and 57.5 degree corresponding to d values of 3.111, 1.899 and 1.622 \AA , respectively. The peaks are identified to originate from (111), (220) and (311) planes of the cubic (zinc blend) phase of ZnS [JCPDS Card No. 36-1450]. The broadening of the diffraction peaks indicates the nanocrystalline nature of the sample. The average crystalline size is calculated from the full width at half maximum (FWHM) of the diffraction peaks using Debye-Scherrer formula [16] $D = k\lambda / \beta \cos \theta$ where D is the mean grain size, k is a geometric factor ($=0.89$), λ is the X-ray wavelength, β is the FWHM of diffraction peak and θ is the diffraction angle. The average grain size of the uncapped and PVA –capped ZnS:Mn²⁺ particles calculated from the three peaks is 4.4 and 2.8 nm. The size of nanocrystals of the sample is thus in the strong charge confinement regime.

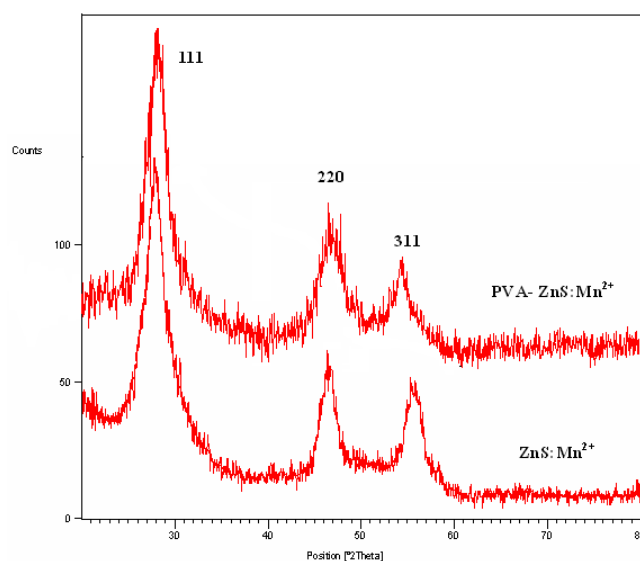


Fig. 1 XRD pattern of uncapped and capped (PVA) ZnS:Mn^{2+} nanoparticles.

Fig. 2 shows the TEM of PVA -capped ZnS:Mn^{2+} nano-particles with the corresponding diffraction pattern. Presence of fine ZnS:Mn^{2+} nano-particles is clearly visible in the TEM picture (Fig. 2(a) & (b)). The diffraction pattern (Fig 2 (c)) of the sample consists of a central halo with concentric broad rings. The rings correspond to the reflections from (111), (220) and (311) planes confirming the cubic structure of the ZnS nano-particles. The average size of the nano-crystallites determined from TEM is around 3 nm. This result is almost consistent with the XRD result.

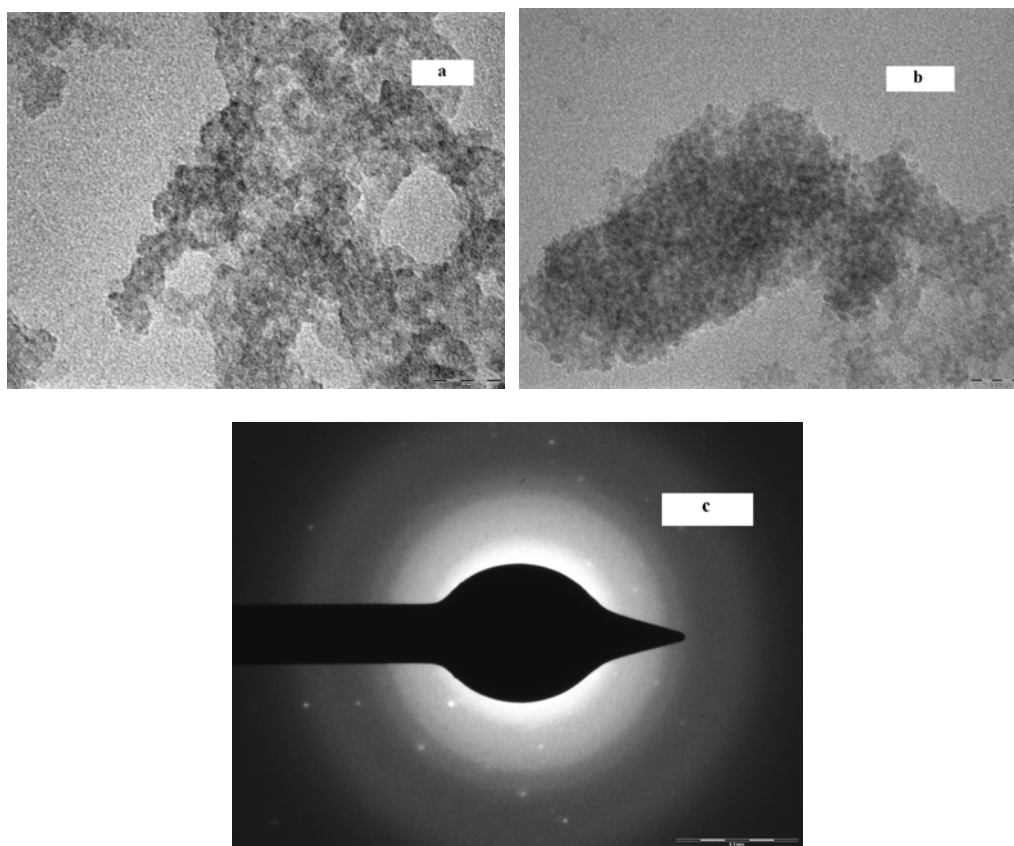


Fig. 2 (a & b) TEM micrograph of PVA -capped ZnS:Mn^{2+} nanocrystals. The scale bar represents 20 nm (c) Shows the SAED pattern of PVA(1.5g) -capped nanocrystals.

The UV/Vis absorbance spectra for freshly-prepared PVA -capped (different concentration) Mn^{2+} -doped (4%) ZnS nanocrystals are shown in Fig. 3. As observed in the figure, the samples exhibit an excitonic peak at around 315 nm for uncapped and 296 nm for PVA -capped ZnS: Mn^{2+} nanoparticles. The variation of the excitation peak position indicates a change of the particles size or influence of the surfactant in prepared solution. These absorption edges of capped ZnS: Mn^{2+} nanoparticles were at shorter wavelength than the 345 nm for bulk, suggesting the formation of nanometer-sized ZnS: Mn^{2+} particles in the samples. [17]. The shifting of absorption edges to shorter wavelength could be explained by the quantum confinement of ZnS: Mn^{2+} nanocrystallites. These absorption spectra have been used to calculate approximate sizes for these nanocrystals using the Brus equation [17]. Based on the peaks position in the absorbance spectra of the uncapped and PVA -capped particles size have been calculated to be ~ 4 nm and 2.6 nm, respectively.

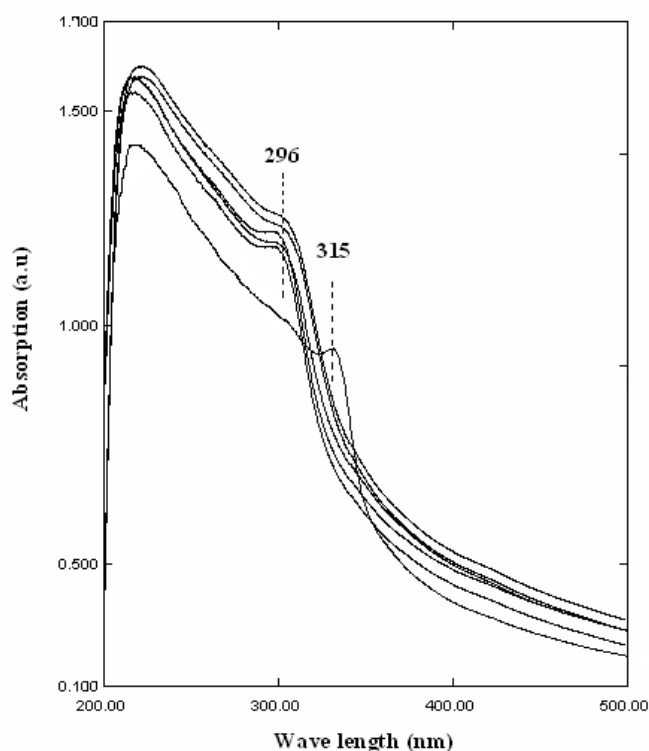


Fig. 3. Absorption spectra of uncapped and PVA -capped ZnS: Mn^{2+} nanoparticles.

Fig. 4 (a) showed the room temperature photoluminescence spectra of ZnS: Mn^{2+} nanocrystals with different concentrations (0.5, 1, 2, 3 and 4%) of Mn^{2+} under 310 nm excitation. For all ZnS: Mn^{2+} samples, two different emission bands dominated the PL spectra. The first emission band at about 460 nm, which could be ascribed to a recombination of electrons at the sulfur vacancy donor level with holes trapped at the zinc vacancy acceptor level. The second emission band was centered at about 580 nm, which was due to ${}^4\text{T}_1 - {}^6\text{A}_1$ transition within the 3d shell of Mn^{2+} [18]. Different groups [8, 19] have studied the origin of the yellow-orange emission from Mn^{2+} in ZnS nanoparticles. Karar et al. [8] reported the synthesis of ZnS: Mn^{2+} nanoparticles with Mn^{2+} concentration varying in the 0-40% range through the chemical method with polyvinylpyrrolidone (PVP) as a capping agent and iso-propanol as the solvent. The size of the prepared nanoparticles was 4 nm [8]. The emission peak at 460 nm was attributed to native impurity sites. The peak at 600 nm was attributed to ${}^4\text{T}_1 - {}^6\text{A}_1$ transition of Mn^{2+} in ZnS [8]. Sapara et al. [19] reported the preparation of ZnS: Mn^{2+} nanoparticles with 2% and 6% Mn-doping through the chemical method. The preparation of sample was done at higher temperature at 100°C, with dimethyl formamide was used as the solvent and 1-thioglycerol as a capping agent. The average

diameter of the prepared nanoparticles was ~ 1.6 nm. They reported 580 nm PL emission from Mn-doped sample due to Mn d-d transition upon 290 nm UV excitation. Mello Donega et al. [20] reported the synthesis of ZnS:Mn²⁺ nanoparticles with 1 and 2.5 mol% Mn-doping through the chemical method. The size of the prepared particles was 4.4 nm. The emission peak at about 425 nm, ascribed to radiative recombination at defects in the ZnS nanocrystals and the emission spectrum consists of a very intense broad band at 590 nm, ascribed due to ${}^4T_1 - {}^6A_1$ transition of the Mn²⁺ ion. Fig. 4 (b) shows the recombination mechanism for the ZnS:Mn²⁺ system.

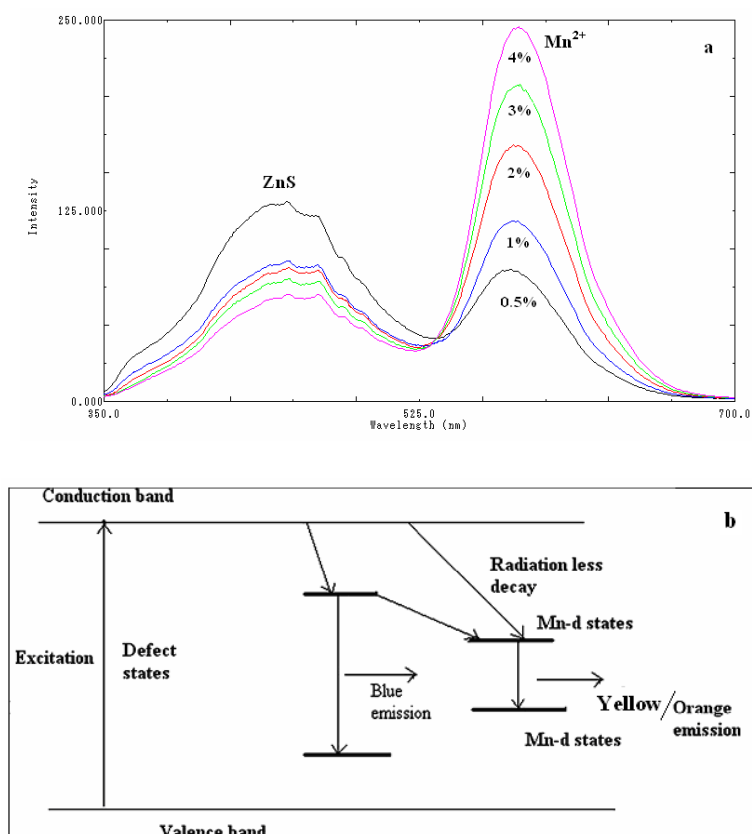


Fig. 4. (a) shows the PL emission spectra of different concentration (0.5 – 4%) of Mn²⁺-doped ZnS nanoparticles. (b) The recombination mechanism for the ZnS:Mn²⁺ system.

Fig. 5 shows the photoluminescence emission spectra of ZnS:Mn/carboxylic PVA nanocomposites. From this, 1.5 g of PVA is optimum concentration for enhanced PL intensity than the other. Comparing the PL properties of the uncapped and capped ZnS:Mn²⁺ nanoparticles, the capped ZnS:Mn²⁺ is having more PL intensity due to control and homogeneous growth of the nanoparticles in prepared solution. The limiting mechanism for particle growth in our system is probably the inhibition of diffusion, since the bending or coiled structures of the polymer chains will hinder the diffusion-driven processes within the network. It is also possible that polymer chains may be bridged by connecting to the same nanoparticle, and a multiplicity of such bridged chains and particles could lead to particle clustering [21]. The higher ionic content in PVA has effected a more efficient clustering of the ionic groups into domains of small size. It is known that the crystalline nature of PVA results from the strong intermolecular interaction between PVA chains through the intermolecular hydrogen bonding. It may be the reason that the interactions between PVA chains and ZnS:Mn²⁺ particles led to the decrease of intermolecular interaction of PVA chains, which would result in decreasing the crystalline degree of PVA and enhanced PL intensity for both emission.

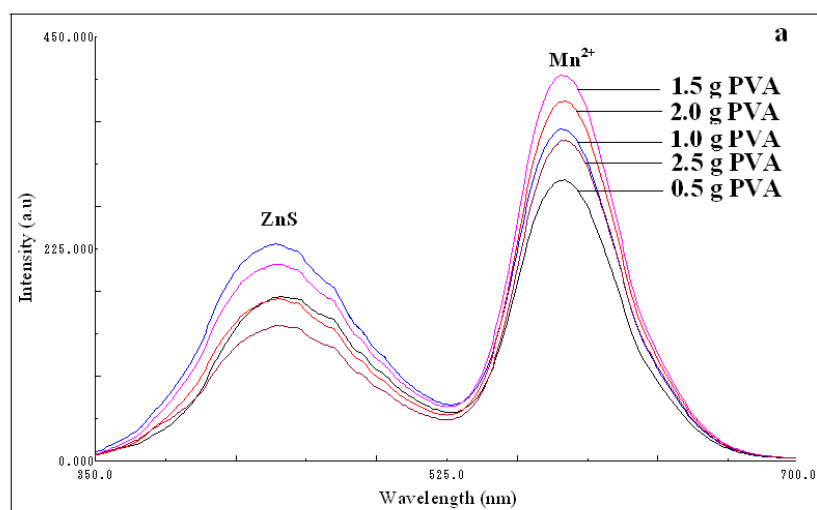


Fig. 5. Shows the PL emission spectrum for different concentration PVA -capped ZnS:Mn²⁺ nanoparticles.

4. Conclusions

Mn²⁺-doped ZnS nanoparticles with enhanced luminescence have been synthesized by chemical precipitation method using PVA as capping agent. The observation of ~50 nm blue shifting (lower wavelength) from bulk in UV studies dictated the quantum confinement effect. The enhanced yellow-orange emission due to Mn²⁺ ⁴T₁-⁶A₁ transition is obtained under the excitation wavelength of 296 nm for capped and 315 nm for uncapped ZnS:Mn²⁺ nanoparticles.

Acknowledgements

The authors thank to Dr. AN. Kannappan, Professor and Head, Department of Physics, Annamalai University for providing laboratory facilities and financial support. The authors also thank Dr. N. Rajendran, Department of chemistry, Annamalai University, for providing PL facility.

References

- [1] C. Burda, X. Chen, R. Narayanan, M.A. El-Sayed, Chem. Rev. **105**, 1025 (2005).
- [2] C.N.R. Rao, G.U. Kulkarni, P.J. Thomas, P.P. Edwards, Chem. Eur. J. **8**, 28 (2002).
- [3] G. Shen, Y. Bando, D. Golberg, Appl. Phys. Lett. **88**, 123107 (2006).
- [4] X. Jiang, Y. Xie, J. Liu, L. Zhu, W. He, Y. Qian, Chem. Mater. **13**, 1213 (2001).
- [5] N.A. Dhas, A. Zaban, A. Gedanken, Chem. Mater. **11**, 806 (1999).
- [6] Y. Zhao, Y. Zhang, H. Zhu, G.C. Hadjipanayis, J.Q. Xiao, J. Am. Chem. Soc. **126**, 6874 (2004).
- [7] Y.Q. Li, J.A. Zapien, Y.Y. Shan, Y.K. Liu, S.T. Lee, Appl. Phys. Lett. **88**, 013115 (2006).
- [8] S. Sapra, A. Prakash, A. Ghangrekar, N. Periasamy, D.D. Sarma, J. Phys. Chem. B **109**, 1663 (2005).
- [9] R.N. Bhargava, D. Gallagher, Phys. Rev. Lett. **72**, 416 (1994).
- [10] A.A. Bol, A. Meijerink, J. Phys. Chem. B **105**, 10203 (2001).
- [11] Y. Zhang, Y. Li, J. Phys. Chem. B **108**, 17805 (2004).
- [12] P. Balaz, Extractive Metallurgy of Activated Minerals, Elsevier, Amsterdam, 2000.

- [13] J. O. Fornell, H. G. Grimmeis, R. Mach, G. O. Muller, *Semicond. Sci. Technol.* **3**, 511 (1988).
- [14] P. Balaz, Z. Bastl, J. Briancin, I. Ebert, J. Lipka, *J. Mater.Sci.* **27**, 653 (1992).
- [15] I. Yu, T. Isobe, M. Senna, *J. Phys. Chem. Solids* **57**, 373 (1996).
- [16] B. D. Cullity, *Elements of X-ray Diffraction*, second ed., Addison-Wesley Company, USA, p.102.
- [17] P. Vinotha Boorana Lakshmi, K. Sakthi Raj, K. Ramachandran, *Cryst. Res. Technol.* **44**, 153 (2009).
- [18] M. Konishi, T. Isobe, M. Senna, *J. Lumin.* **93**, 1 (2001).
- [19] K. Manzoor, S. R. Vadera, N. Kumar. T. R. N. Kutty, *Mater. Chem. Phys.* **82**, 718 (2003).
- [20] C. De. M. Donega, A. A. Bol, A. Meijerink, *J. Lumin.* **96**, 87 (2002).
- [21] H. Du, G. Q. Xu, W. S. Chin, L. Huang, W. Ji, *Chem. Mater.* **14**, 4473 (2002).